Applied Catalysis B: Environmental 148–149 (2014) 582–588

Contents lists available at ScienceDirect

Applied Catalysis B: Environmental

journal homepage: www.elsevier.com/locate/apcatb

The role of cerium in the improved SO_2 tolerance for NO reduction with NH_3 over Mn-Ce/TiO_2 catalyst at low temperature

Ruiben Jin[a,b], Yue Liu[a,*], Yan Wang[a], Wanglai Cen[a], Zhongbiao Wu[a], Haiqiang Wang[a], Xiaole Weng[a]

[a] Department of Environmental Engineering, Zijingang Campus, Zhejiang University, Yuhangtang Road 388, Hangzhou 310058, PR China
[b] Environmental Science &Design Research Institute of Zhejiang Province, Tianmushan Road 111, Hangzhou 310027, PR China

ARTICLE INFO

Article history:
Received 26 April 2013
Received in revised form 4 September 2013
Accepted 16 September 2013
Available online 26 September 2013

Keywords:
Nitrogen oxides
SCR
Low-temperature
DRIFT
SO_2 tolerance

ABSTRACT

Manganese-based catalysts have shown excellent low-temperature selective catalytic reduction (SCR) activity for NO_x removal. However, they all suffer from the serious SO_2 poisoning effect on activity. Ceria modification has been reported to be able to promote SO_2 tolerance of SCR catalysts probably via the inhibition of surface sulfate species formation. In this study, *in situ* diffuse reflectance infrared transform spectroscopy (DRIFT) investigations were carried out to determine the role of Ceria in the improved resistance for a Ce-modified Mn/TiO_2 catalyst. The results indicated that after the introduction of Ce, SO_x ad-species preferentially formed on Ceria as bulk-like sulfate species and lessened the sulfation of the main active phase (MnO_x) during low-temperature SCR processes in the presence of SO_2. Furthermore, the DRIFT and TG–DSC results also implied that Ce modification could reduce thermal stabilities of the sulfate species covered on catalyst surface, thereby promoting its decomposition. Both of these would be beneficial to the improved SO_2 tolerance of Ce modified catalysts.

1. Introduction

Selective catalytic reduction (SCR) of NO_x with NH_3 is an effective process for removing NO_x from stationary sources, whereas most commercial catalysts for this process are V_2O_5/TiO_2 promoted by WO_3 or MoO_3 [1,2]. Generally, to avoid the deposition of dust on catalysts, the SCR reactor is preferred to be located downstream of the particle controller, where the temperature of flue gas is usually below 300 °C (this is lower than the active temperatures of commercial SCR catalysts). As such, it is necessary to reheat the flue gas, which unfavorably affects the economics of SCR, however. For this reason, there has been strong interest in developing a superior SCR catalyst with high activity at low temperature range [3].

Recently, Mn-containing catalysts have attracted a lot of research attention for their superior activity in low-temperature SCR reactions [4–9]. Manganese oxides contain various types of labile oxygen, which is beneficial to the fulfillment of the catalytic cycle [10]. We have also reported Mn/TiO_2-based catalysts prepared by the sol–gel method that have high activity at low temperature [11,12]. These works have resolved the activity problem for low-temperature SCR catalysts. However, there is still certain amount of SO_2 in the flue gas or exhausted gas, which could have a serious poisoning effect on SCR catalytic activity in the low temperature range [13–15]. The deactivation of Mn-based catalysts caused by SO_2 was proposed due to two main aspects described in previous reports [16–18]. First, SO_2 would react with NH_3 to form NH_4HSO_4, which did not decompose at low temperature and deposited on the catalyst surface, blocking the active sites of the SCR catalysts. Second, the active phase, such as MnO_x, was sulfated by SO_2 and formed stable sulfate species, which were inactive in the SCR reaction. As such, insight into improving sulfur tolerance of the low-temperature SCR catalysts has attracted wide concern [19–22].

Chang et al. [19] reported that the addition of Sn into MnO_x-CeO_2 catalysts via a co-precipitation method greatly enhanced SO_2 resistance owing to the enhanced Lewis acid sites during SO_2-containing SCR reaction. Shen et al. [20] proposed that iron doping would have a positive effect of SO_2 tolerance of Mn-Ce/TiO_2, because iron oxide significantly decreased the rate of sulfate formation. Yu et al. [21] argued that the catalyst structure rather than the catalyst composition dominated the catalyst's resistance to the poisoning of SO_2 during SCR of NO with NH_3 at low temperature. Furthermore, the mesoporous structure facilitated SO_2 resistance compared to microporous structure. We have also found that Ce doping can greatly improve the SO_2 resistance of Mn-Ce/TiO_2 catalysts [23] because both the accumulation of ammonium sulfates and the active phase sulfation were reduced to a great extent. Similar findings were obtained in a previous study [24]. However, the inherent

* Corresponding author. Tel.: +86 571 87953088; fax: +86 571 87953088.
E-mail address: yueliu@zju.edu.cn (Y. Liu).

0926-3373/$ – see front matter © 2013 Elsevier B.V. All rights reserved.
http://dx.doi.org/10.1016/j.apcatb.2013.09.016

role of Ce doping in these changes regarding the decrease in the formation of surface sulfation species was still unclear. Furthermore, the pore diameter showed little difference after Ce doping [12], indicating that the enhanced SO_2 resistance was not due to changes in micro-structures.

Therefore, in this study, further work was conducted to investigate the role of Ce addition in SO_2 tolerance enhancement. We expect that the results present herein will be helpful in developing high-activity SCR catalysts with excellent SO_2 resistance in a low temperature range.

2. Experimental

2.1. Catalyst preparation

The catalyst was prepared by the sol–gel method as we previously reported [23]. Tetrabutyl titanate (0.1 mol), manganese nitrate (0.04 mol), ethanol (0.8 mol), water (0.6 mol) and acetic acid (0.3 mol) were mixed under vigorous stirring at room temperature to form a transparent sol. During this process, 0.01 mol of cerium nitrate was added for the preparation of Mn-Ce/TiO_2 catalyst. The sol transformed to a gel after stabilization at room temperature for two weeks. The gel was dried at 110 °C to remove organic solvents. Then, the solid was crushed and sieved to 40–60 mesh and calcined at 500 °C in air for 6 h in a tubular furnace.

2.2. Catalytic activity measurement

SCR activity measurements were carried out in a fixed-bed at 150 °C containing 2 mL catalyst with a gas hourly space velocity (GHSV) of 40,000 h^{-1}. The reactant gas typically consisted of 800 ppm NO, 800 ppm NH_3, 3% O_2, 100 ppm SO_2 (when used), 3 vol% water and balance N_2. The reactants were pre-heated in a gas mixer, and then, the mixed gas was sent to the reactor. Water vapor was generated by passing N_2 through a heated gas-wash bottle (80 °C) containing deionized water. The concentrations of NO and NO_2 were monitored by a NO–NO_2–NO_x analyzer (Thermo, Model 42i-HL), while the concentration of SO_2 was monitored by a SO_2 analyzer (Thermo, Model 43i-HL).

2.3. FT-IR study and TG–DSC measurements

FT-IR spectra were acquired using an *in situ* DRIFT cell equipped with gas flow system. The DRIFT measurements were performed with ZnSe windows coupled to Nicolet 6700 FTIR spectrometers. In the DRIFT cell, the catalyst was pretreated at 500 °C in He environment for 2 h and then cooled to 150 °C. The background spectrum, recorded under flowing He, was subtracted from the sample spectrum. The final differential sample spectra were calculated by Kubelka–Munk function. Thermogravimetric analysis (TG) and differential scanning calorimetry (DSC) analysis were carried out to investigate the thermal stability of sulfate species over the Mn/TiO_2 and Mn-Ce/TiO_2 catalysts. Fresh catalyst was first dipped into the solution of NH_4HSO_4 (1 mol/L) for 12 h and then was dried at 100 °C overnight to remove water. Finally, TG and DSC experiments were carried out simultaneously in a static N_2 atmosphere, using a Netzsch STA 409 instrument. For each experiment, 12–15 mg of each sample was analyzed between 35 and 800 °C at a rate of 10 K/min.

3. Results and discussion

3.1. SCR performance

The effect of SO_2 on SCR activity of Mn/TiO_2 and Mn-Ce/TiO_2 is illustrated in Fig. 1. It can be observed that the NO conversion

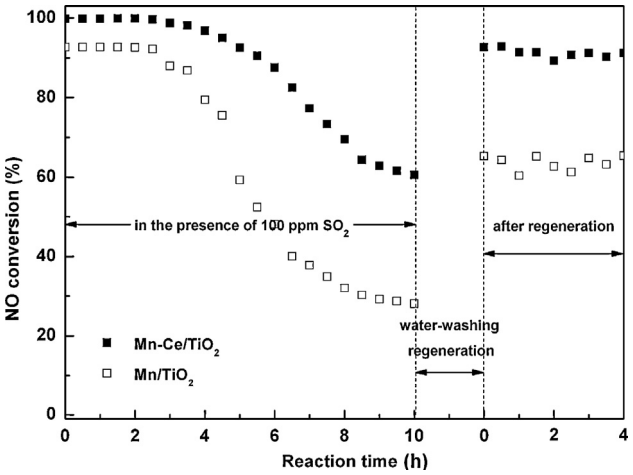

Fig. 1. SCR activities of Mn/TiO_2 and Mn-Ce/TiO_2 in the presence of SO_2 at 150 °C. ([NH_3] = [NO] = 800 ppm, [O_2] = 3%, [SO_2] = 100 ppm, [H_2O] = 3 vol%, N_2 balance, GHSV = 40,000 h^{-1}).

of the Mn/TiO_2 catalyst decreased much more rapidly than that of the Mn-Ce/TiO_2 catalyst. Only 25% of NO conversion was retained by Mn/TiO_2 after 10 h, while approximately 60% of NO conversion by Mn-Ce/TiO_2 remained under the same reaction conditions. The used catalysts were then generated by washing with deionized water followed by dying at 105 °C for 12 h. The NO conversion of Mn-Ce/TiO_2 could be recovered to above 90% after regeneration, while the regenerated Mn/TiO_2 only yielded approximately 60% NO conversion. As mentioned in the introduction section, a SO_2 deactivation mechanism for NH_3-SCR catalysts has been reported to be due to the sulfation of the active phase and the deposition of ammonium sulfate/bisulfate, which could be easily removed by water washing. Therefore, this result implied that Ce doping could greatly lessen the sulfation of MnO_x during SCR reaction in the presence of SO_2.

3.2. In-situ DRIFT analysis

3.2.1. SO_2 adsorption on Mn/TiO_2 and Mn-Ce/TiO_2 catalysts

Fig. 2 shows the DRIFT spectra of adsorbed species over Mn/TiO_2 and Mn-Ce/TiO_2 catalysts in flowing $SO_2 + O_2$ at 150 °C as a function of time and then purged with He for 30 min. As shown in Fig. 2A, several peaks at 975, 1074, 1137, 1179, 1240, 1375, 1425 and 1629 cm^{-1} were detected for NH_3 adsorption on the Mn/TiO_2 catalyst, and the intensities increased with time. All of these bands could be assigned to the sulfate species formed on the catalyst [25]. The bands at 1425 and 1375 cm^{-1} corresponded to surface sulfate species [26], and the peaks at approximately 1200 cm^{-1} (1240, 1179 cm^{-1}) were attributed to bulk-like sulfate species [27,28]. Other peaks could be assigned to either surface or bulk-like sulfates because the IR bands were strongly overlapped within the range of 900–1150 cm^{-1} for both types of sulfate species [25]. Moreover, the band at 1629 cm^{-1} was assigned to adsorbed H_2O due to the reaction of SO_2 and surface hydroxyl groups [29], which was weakened after He purging for 30 min. Overall, both surface and bulk-like sulfate species could be formed on Mn/TiO_2 after treatment with SO_2. However, the IR spectrum of the Mn-Ce/TiO_2 catalyst after the introduction of SO_2 and O_2 was quite different compared with that of the Mn/TiO_2 catalyst (Fig. 2B): It showed a strong broad band at approximately 1185 cm^{-1}. According to Waqif et al.'s results [26], the bulk-like sulfation species are characterized by a broad band at approximately 1200 cm^{-1}. Therefore, this broad band could be assigned to the bulk-like sulfate species formed over Mn-Ce/TiO_2. In addition, there were no surface species (characterized bands at

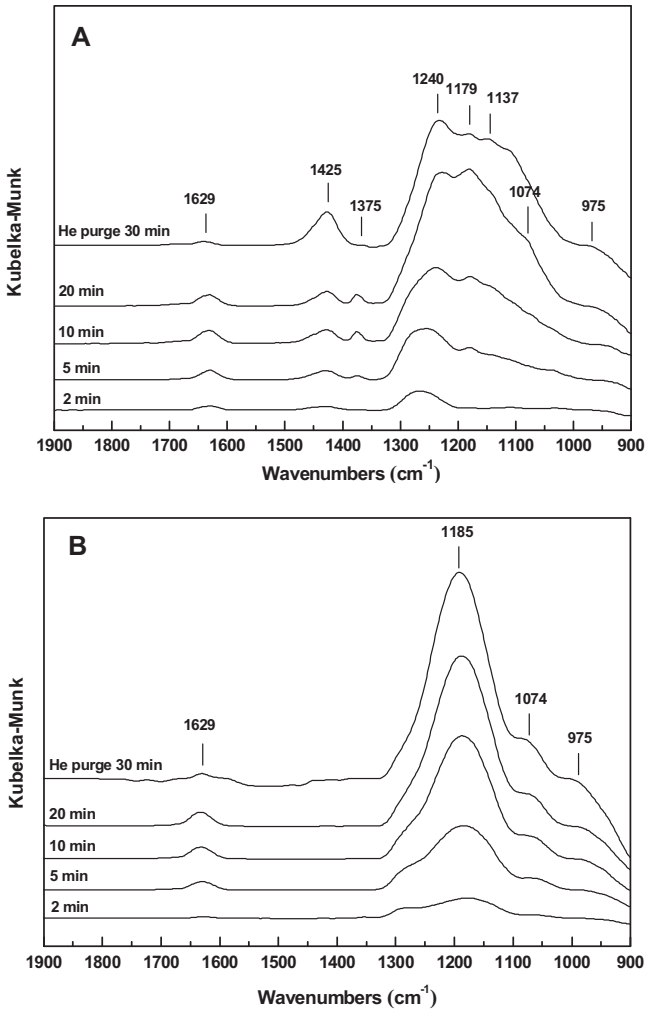

Fig. 2. DRIFT spectra of Mn/TiO_2 (A) and $Mn\text{-}Ce/TiO_2$ (B) exposed to 100 ppm SO_2 in the presence of O_2 for various times and subsequently purged by He for 30 min at 150 °C.

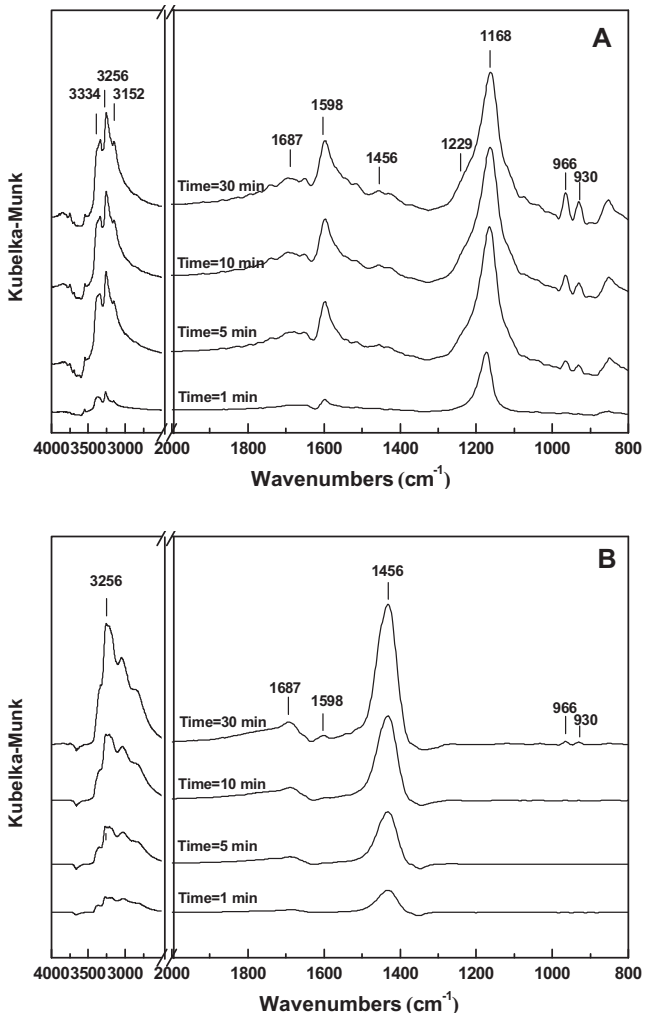

Fig. 3. DRIFT spectra of NH_3 adsorption on fresh (A) and pre-treated (B) Mn/TiO_2 for various times at 150 °C.

1400–1350 cm^{-1}) detected in the IR spectrum of the $Mn\text{-}Ce/TiO_2$, which indicated that the addition of Ceria might partially prevent active sites of sample from being sulfated. Because Ceria is basic material for SO_2 adsorption [26], sulfate species might preferentially form on Ceria dopants, lessening the sulfation of MnO_x sites.

3.2.2. NH_3 adsorption on fresh catalysts and catalysts pretreated by SO_2

In this section, Mn/TiO_2 and $Mn\text{-}Ce/TiO_2$ catalysts were both first exposed to 100 ppm SO_2 in the presence of O_2 for 30 min followed by He purging and scanned as background spectrum. Then, NH_3 was introduced and the IR spectra were recorded as a function of time. NH_3 adsorption on fresh samples was also investigated for comparison.

As illustrated in Fig. 3A the introduction of NH_3 onto fresh Mn/TiO_2 led to the formation of peaks at 930, 966, 1168, 1456, 1598 and 1687 cm^{-1} in the low wavenumber region. The strong band at 1168 cm^{-1} with a shoulder at 1229 cm^{-1} was a result of the symmetric deformation of NH_3 ($\delta_s(NH_3)$) coordinatively bound to Lewis acid sites [30–32]. The moderate band at 1598 cm^{-1} was due to coordinated NH_3 on Lewis acid sites [11,33]. Two weak bands at 1456 and 1687 cm^{-1} were attributed to $\delta_{as}(NH_4^+)$ and $\delta_s(NH_4^+)$ bound to Brønsted acid sites, respectively [30–32,34]. The band at 930 and 966 cm^{-1} was assigned to weakly adsorbed NH_3 or gas-phase NH_3 according to our previous work [11]. In the high wavenumber region, peaks were observed at 3152, 3256 and 3334 cm^{-1}. The bands at 3152 and 3256 cm^{-1} were assigned to symmetric stretching of NH_3 coordinated to Lewis acid sites ($\upsilon_s(NH_3)$), while the peak at 3334 cm^{-1} was due to $\upsilon_{as}(NH_3)$ coordinated to Lewis acid sites [30–32,34].

Fig. 3B clearly shows the dominant presence of Brønsted acid sites on pre-treated Mn/TiO_2. The initial peaks at 1168 and 1229 cm^{-1} disappeared and the band at 1598 cm^{-1} was sharply weakened. These peaks were assigned to coordinated NH_3 on Lewis acid sites. While the band at 1456 and 1687 cm^{-1} due to NH_4^+ species bound to Brønsted acid sites [30–32,34] could still be observed on pre-treated Mn/TiO_2 catalyst, the peak at 1456 cm^{-1} was significantly strengthened. These results suggest that the formed sulfate species on Mn/TiO_2 surface could produce new Brønsted acid sites but sharply weakened the Lewis acidity of catalyst. However, the ammonium adsorbed on Brønsted acid sites was believed to mainly react with adsorbed nitrite, nitrate species or NO_2 [35,36] in a low temperature range, and the presence of SO_2 would strongly restrain the adsorption and oxidation of NO (this will be discussed in Section 3.2.3). Therefore, the increase of Brønsted acidity after SO_2 adsorption contributes little to the SCR activity for Mn/TiO_2 catalyst at low temperature range.

DRIFT spectra of NH_3 on fresh $Mn\text{-}Ce/TiO_2$ and sulfated $Mn\text{-}Ce/TiO_2$ have been reported in Fig. 6 (A and B) of our previous study [37]. It was reproduced herein as Fig. 4 for the comparison with the

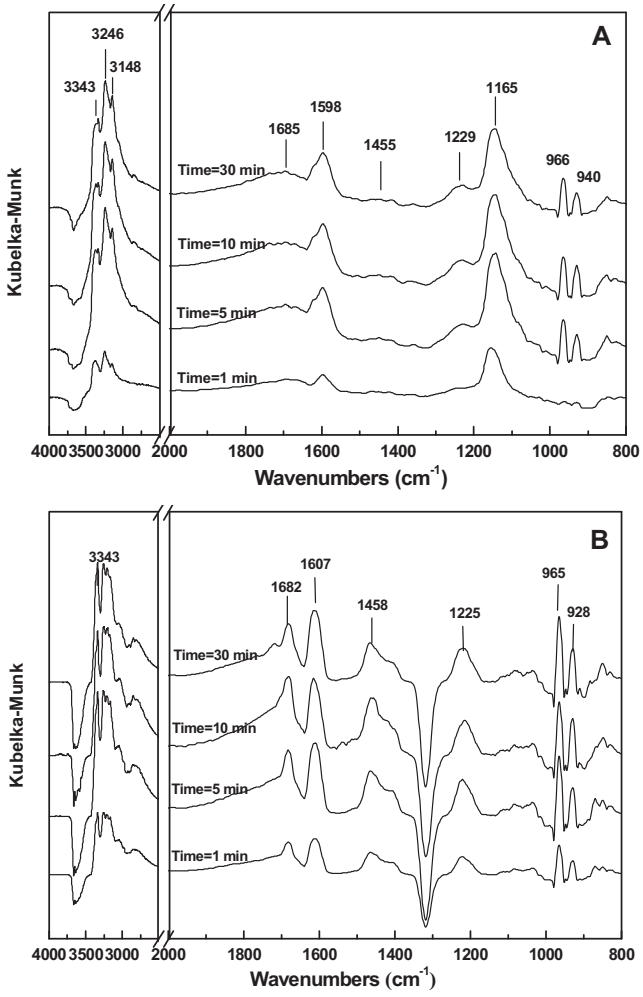

Fig. 4. DRIFT spectra of NH_3 adsorption on fresh (A) and pre-treated (B) Mn-Ce/TiO_2 for various times at 150 °C (reproduced from the Ref. [37]).

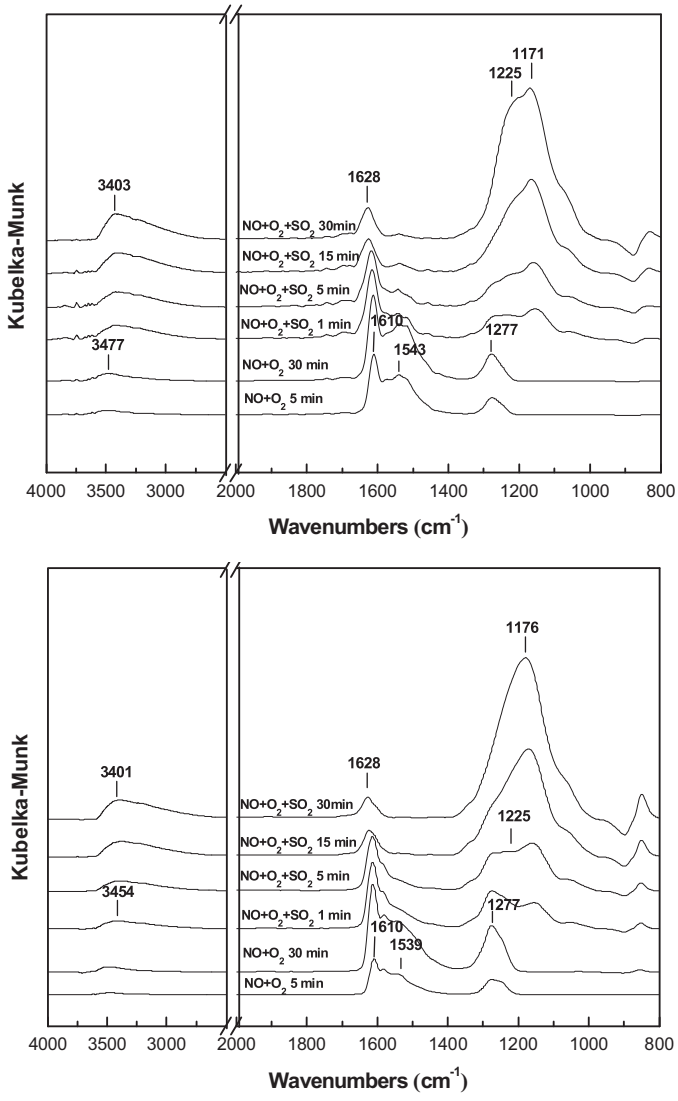

Fig. 5. DRIFT spectra of Mn/TiO_2 (A) and Mn-Ce/TiO_2 (B) exposed to 800 ppm NO in the presence of O_2 followed by the introduction of 100 ppm SO_2 at 150 °C.

results for Mn/TiO_2 shown in Fig. 3. In Fig. 4A, the peaks at 1165, 1229, 1455, 1598 and 1688 cm^{-1}, which existed for Mn/TiO_2 could also be detected on the DRIFT spectra for fesh Mn-Ce/TiO_2. The peaks assigned to NH_4^+ species bound to Brønsted acid sites (1682 and 1458 cm^{-1}) were also amplified on pre-treated Mn-Ce/TiO_2 as shown in Fig. 4B. However, the Lewis acidity of the pre-treated Mn-Ce/TiO_2 was quite different from that of the pre-treated Mn/TiO_2 catalyst. The bands due to coordinated NH_3 on Lewis acid sites (1607 and 1225 cm^{-1}) still existed on the pre-treated Mn-Ce/TiO_2 surface. This finding implied that the sulfation of Lewis acid sites could be effectively restrained on the catalyst surface by Ce doping, which also supported that the sulfation of MnO_x was weakened after Ce addition. In addition, a portion of Lewis acid sites were preserved, which would be beneficial to maintaining the SCR activity to some extent at low temperature in the presence of SO_2. Furthermore, the negative peak at approximately 1320 cm^{-1} in Fig. 4B was assigned to (S=O) bond due to the interaction between sulfate species and NH_3 based on the previous study [38].

3.2.3. *Competitive adsorption between SO_2 and NO on catalysts' surface*

Because both of SO_2 and NO are acidic gases, they are apt to be adsorbed on the same active sites on a catalyst's surface. Therefore, it is necessary to investigate the competitive adsorption between SO_2 and NO on each catalyst's surface.

As described in this section, catalysts were first exposed to NO in the presence of O_2, and then, SO_2 was introduced to the gas system. When NO was adsorbed on the Mn/TiO_2 and Mn-Ce/TiO_2 surfaces for 30 min, four peaks located at 3477/3454, 1610, 1543/1539 and 1277 cm^{-1} were observed in both catalysts' DRIFT spectra, as illustrated in Fig. 5. The band at 3477/3454 cm^{-1} was assigned to O–H stretching in NOH groups [39]. The peaks at 1610 and 1543/1539 cm^{-1} were attributed to bridge and bidentate nitrate species, respectively [40,41], And the peak at 1277 cm^{-1} corresponded to monodentate nitrate species [42]. After SO_2 was introduced for 30 min, the initial peaks due to nitrate species vanished, and new bands at 1628 and 1171/1176 cm^{-1} were formed for both catalysts. These two new peaks corresponded to weakly adsorbed sulfate species [28]. Another new band at 1225 cm^{-1} was obtained on the Mn/TiO_2 surface, which was due to adsorbed bidentate sulfate [27]. The results shown in Fig. 5 clearly indicated that there was competitive adsorption between SO_2 and NO on both of the catalysts and that the adsorption ability of SO_2 was much higher than NO. Consequently, we can propose that NO would be weakly adsorbed on the surface of Mn/TiO_2 or Mn-Ce/TiO_2 catalysts in the presence of SO_2. These results implied that there was no occurrence of the SCR reaction between the adsorbed NO_x species and

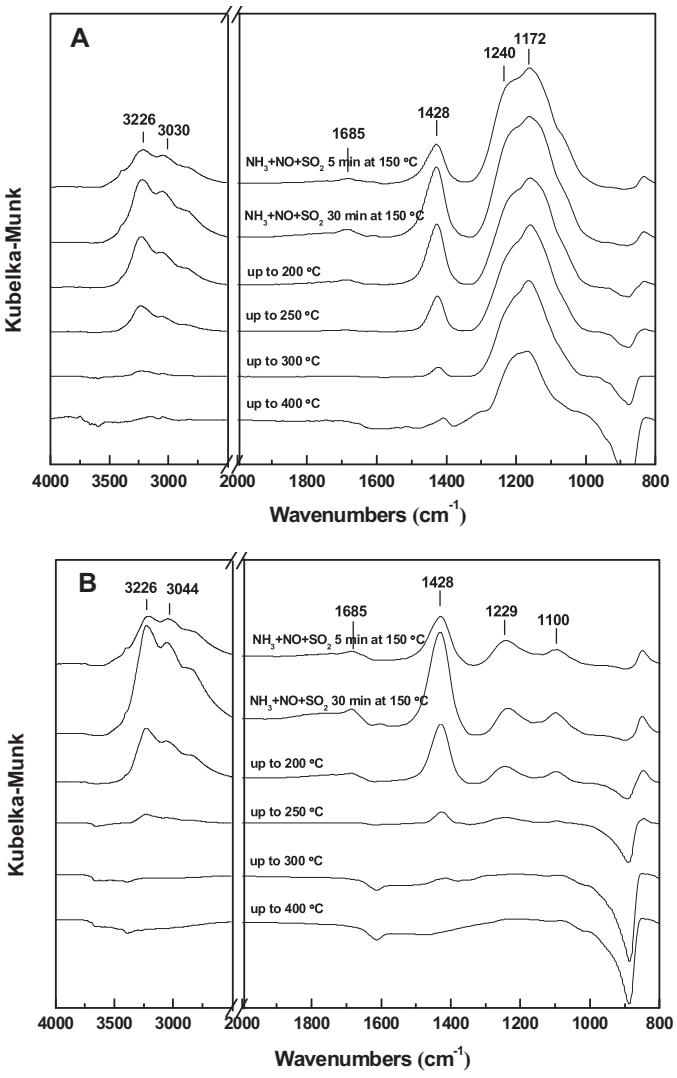

Fig. 6. DRIFT spectra of Mn/TiO_2 (A) and $Mn\text{-}Ce/TiO_2$ (B) exposed to 800 ppm NH_3 + 800 ppm NO + 100 ppm SO_2 in the presence of O_2 for various times at 150 °C. Subsequently, the atmosphere was switched to only He and the temperature was escalated to 400 °C.

adsorbed NH_3 species through L–H mechanism in the presence of SO_2, which may have also decreased the total NO conversion.

3.2.4. *Thermal stability of surface species on catalysts surface during SCR process*

To understand the SCR reaction behaviors in the presence of SO_2, further investigations into the thermal stability of the formed sulfate species over the surface of Mn/TiO_2 and Ce doped Mn/TiO_2 were carried out by *in-situ* DRIFT experiments, where the SO_2, NH_3 and NO were introduced to the system synchronously. Peaks at 1685, 1428, 1240 and 1172 cm^{-1} were detected on the Mn/TiO_2 surface, as shown in Fig. 6A. As we discussed above, the band at 1685 cm^{-1} was due to NH_4^+ bound to Brønsted acid sites, and the peak at 1428 cm^{-1} was also attributed to the NH_4^+ species overlapped by sulfate species, while the other peaks were all related to adsorbed sulfate species. In the case of $Mn\text{-}Ce/TiO_2$ (Fig. 6B), similar bands at 1685, 1428 and 1100 cm^{-1} were detected. The band at 1229 cm^{-1} detected for $Mn\text{-}Ce/TiO_2$ might have been assigned to NH_3 coordinated to Lewis acid sites, which could also have been overlapped by sulfated species. No bands corresponding to nitrate species were detected for either catalyst. Then, the atmosphere was switched from an $NH_3/NO/SO_2$/He mixture to only He, and the temperature was raised from 150 to 400 °C. As shown in Fig. 6A, the peak at 1685 cm^{-1} completely vanished at temperatures higher than 250 °C, and the peaks at 1428, 1240 and 1172 cm^{-1} gradually decreased as the temperature rose; however, they could still be observed at 400 °C. As for $Mn\text{-}Ce/TiO_2$, these bands decreased more quickly and finally disappeared at 400 °C, implying that the formed sulfate species on $Mn\text{-}Ce/TiO_2$ surface decomposed much more easily than those on Mn/TiO_2 surface. According to the literature [3,16,43] and our previous study [23], the deposition of ammonium sulfate species (NH_4HSO_4 and/or $(NH_4)_2SO_4$) and sulfation of active phase during NH_3-SCR process may lead to the deactivation of the SCR catalyst at low temperature. The lower thermal stability of the sulfation species on $Mn\text{-}Ce/TiO_2$ may lead to an increase in its sulfur tolerance.

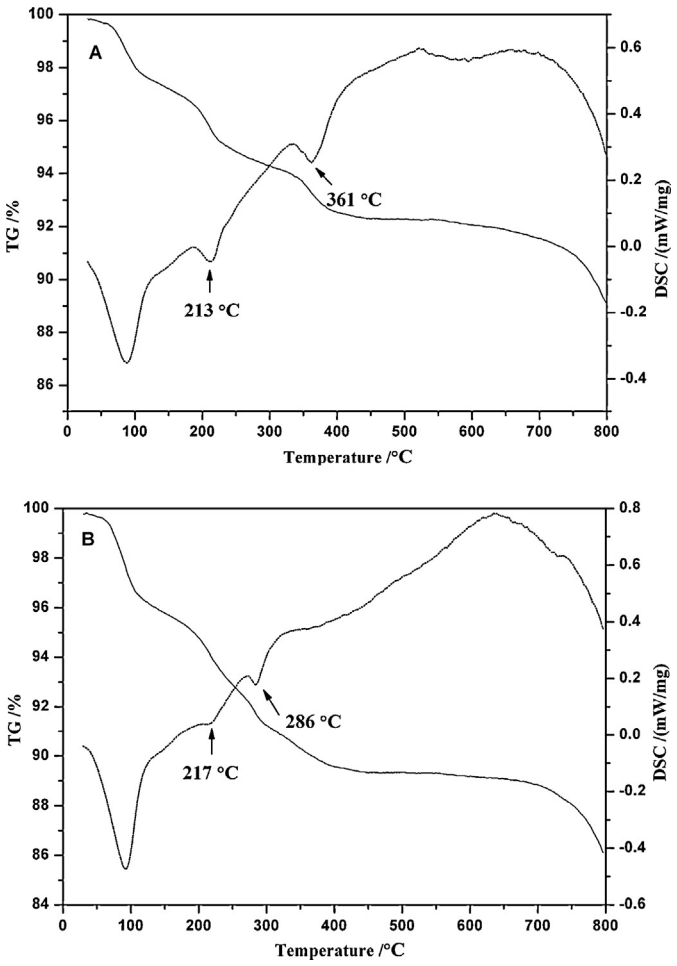

Fig. 7. TG and DSC curves of NH_4HSO_4 deposited on Mn/TiO_2 (A) and $Mn\text{-}Ce/TiO_2$ (B) catalysts.

To further confirm this finding, the thermal stability of the NH_4HSO_4 species on Mn/TiO_2 and $Mn\text{-}Ce/TiO_2$ catalysts was evaluated in the TG/DSC experiments. As shown in Fig. 7A, the TG curve presented three major weight losses and the DSC curve displayed three corresponding valleys for Mn/TiO_2 catalyst. The first one appeared at approximately 90 °C, which was due to the evaporation of water [44]. The other two apparent DSC valleys emerged at 213 and 361 °C, which were close to the decomposition temperatures of $(NH_4)_2SO_4$ (230 °C) and NH_4HSO_4 (350 °C), as reported in the literature [45]. As illustrated in Fig. 7B, in the case of the $Mn\text{-}Ce/TiO_2$ catalyst, the valley due to NH_4HSO_4 decomposition appeared at much lower temperature (at approximately 286 °C) than that on the Mn/TiO_2 catalyst. This finding indicated that the thermal stability of NH_4HSO_4 on $Mn\text{-}Ce/TiO_2$ catalyst was greatly

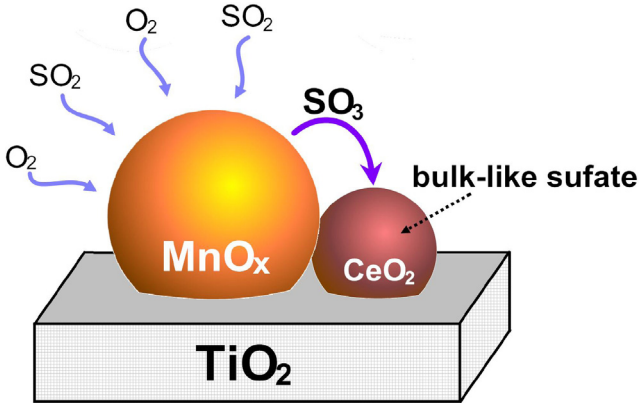

Scheme 1. The formation pathway of bulk-like sulfate on Mn-Ce/TiO_2 samples.

reduced relative to that of Mn/TiO_2, which was well fitted with the DRIFT results.

3.3. Mechanism of the improved SO_2 resistance of Mn/TiO_2 catalyst by Ce doping

According to the FT-IR results mentioned above, it was found that after the introduction of Ce, SO_2 exposure mainly resulted in the formation of bulk-like sulfate species, while both surface and bulk-like sulfate species were formed on Ceria free catalyst (*i.e.*, Mn/TiO_2 catalyst). In our previous study [12], the XPS results of M2p for Mn/TiO_2 and Mn-Ce/TiO_2 before and after SO_2 poisoning showed that the main peak of the Mn 2p3/2 state shifted to higher binding energy (0.7–0.8 eV higher) after SO_2 poisoning. However, for the Ce-doped Mn/TiO_2 catalyst, the binding energy of Mn 2p3/2 did not change. Thus, it can be concluded that the introduction of Ce inhibited the formation of manganese sulfate on catalyst surface. Furthermore, it was reported that Ceria can act as a SO_2 trap for NO_x storage catalysts to limit sulfation of the main active phase when it is exposed to SO_2 [46,47]. Therefore, it was reasonable to deduce that the bulk-like SO_x ad-species formed were mainly stored in Ceria rather than that in MnO_x for the Mn-Ce/TiO_2 catalyst. Furthermore, in Waqif et al.'s experimental work [26], it was demonstrated that the full bulk-like sulfate species on Ceria would only form at a temperature higher than 300 °C during exposure to SO_2 and O_2. However, as our results showed, full bulk-like sulfate species could form over the Mn-Ce/TiO_2 catalyst at a temperature of 150 °C. Considering the very good low-temperature catalytic activity of MnO_x [11], the bulk-like sulfate species were proposed to form via the pathway shown in Scheme 1.

First, SO_2 were catalytically oxidized into SO_3 or sulfation species on MnO_x. Then, SO_3 and sulfation species were adsorbed by or move into Ceria to form bulk-like sulfate species, thereby lessening the sulfation of catalyst active sites (MnO_x). In analogy with V_2O_5/AC catalysts [48], SO_2 was oxidized into SO_3 on V_2O_5 and was stored in active carbon supporter. Kylhammar et al. [47] also concluded that the formation rate of bulk sulfate was more rapid for the Pt/CeO_2 sample compared to the CeO_2 sample. They attributed this result to a higher SO_2 oxidation rate for Ceria compared to that of Pt. Therefore, the sulfation of MnO_x was reduced and Lewis acid sites were preserved to a certain extent (see Fig. 4), as sulfation would normally induce Brønsted acid sites and inhibit Lewis acid sites [37]. As we mentioned above, the SCR reaction through the L-H mechanism was greatly inhibited and Brønsted acid sites contributed little to SCR performance in the presence of SO_2 at low temperature. The adsorption and activation of Lewis acid sites was considered the key step for the low-temperature SCR reaction [30,49]. NH_3 adsorbed on Lewis acid sites could react with gas-phase NO to carry out the SCR reaction at low temperature. This is one of the reasons that Ce addition can greatly improve the SO_2 tolerance of the catalysts. The activity test (see Fig. 1) showed that the SCR activity was almost recovered for Ce-modified catalyst after washing out the ammonium sulfate species covering the catalyst surface. However, the activity could not be fully recovered for Ce-free one. This result also confirmed that sulfation of MnO_x was greatly inhibited after Ce doping. Moreover, because more SO_x ad-species were stored in Ceria, less ammonium sulfate species were formed to cover the surface of Mn-Ce/TiO_2 catalyst during SCR process, which was confirmed in our previous study [12].

The DRIFT and TG–DSC results (see Figs. 6 and 7) also indicated that the thermal stability of sulfation species over Ce-modified catalyst was lower than that over the Ce-free catalyst. As for the surface sulfation species, Kylhammar et al. [47] proposed that the high mobility of sulfates in Ceria would lead to the reversed spillover of sulfates from bulk Ceria to the interface with Pt, resulting in decreases in desorption temperature of these sulfur oxide species. Similarly, it is possible that the bulk sulfation species in Ceria would be more mobile and facilitate their desorption. We also performed a first-principles study to qualitatively determine its stability on both samples using VASP4.6 [50,51] with the GGA + PW91 exchange-correlation functional. It should be noted that to simplify the calculations, we used the Ce-doped MnO_2(1 1 0) slab as the model catalyst, which does not have the true geometric structure of Mn-Ce/TiO_2 catalyst. The results (see Fig. S1) and the details of the calculation method are provided in the supporting information section. From the calculations, it was found that the dissociation energy of NH_4HSO_4 on a pure MnO_2 surface was approximately 0.69 eV, while the corresponding energy on the Ce-doped MnO_2 surface was approximately 0.56 eV. The Ce doping resulted in an approximately 0.13 eV decrease for the surface ammonia sulfate species decomposition. These calculations might provide some theoretical support that Ce doping did reduce the thermal stability of NH_4HSO_4 on Mn-Ce/TiO_2 compared to that on Mn/TiO_2. This is another reason why fewer sulfate species were found to be deposited on the surface of Mn-Ce/TiO_2 than on Mn/TiO_2 under the same reaction conditions, which also contributed to the improved sulfur tolerance of Mn-Ce/TiO_2.

4. Conclusions

In our previous study [23], Ce-doped Mn/TiO_2 showed a remarkable enhancement in its SO_2 tolerance during low-temperature SCR processes, where the accumulation of ammonium sulfates and active phase sulfation was greatly inhibited after Ce doping. The inherent reasons of Ce doping accounting for these changes have been discovered in this study. It was found that surface sulfates were preferentially formed on Ce dopants during the SCR reaction in the presence of SO_2, less sulfation of the main active phase, MnO_x, occurred, and a portion of the Lewis acid sites on MnO_x were preserved to fulfill the low-temperature SCR cycle. The computational results indicated the doping of Ce reduces the binding energy between the NH_4^+ and sulfate ions, which may result in the easier decomposition of ammonium sulfates. The TG–DSC results also confirmed that the decomposition temperature of NH_4HSO_4 on Mn-Ce/TiO_2 was approximately 70 °C lower than that on Mn/TiO_2. All of these results showed that Ce doping could efficiently retard the formation of surface sulfation species, leading to the improvement of sulfur tolerance of Ceria modified catalysts.

Acknowledgments

This project was financially supported by the National Natural Science Foundation of China (No. 51008277), Changjiang Scholar

Incentive Program and Key Project of Zhejiang Provincial Science and Technology Program (2012C03003-4).

Appendix A. Supplementary data

Supplementary data associated with this article can be found, in the online version, at http://dx.doi.org/10.1016/j.apcatb.2013.09.016.

References

[1] H. Bosch, F. Janssen, Catal. Today 2 (1988) 369–379.
[2] S.T. Choo, S.D. Yim, I.S. Nam, S.W. Ham, J.B. Lee, Appl. Catal., B 44 (2003) 237–252.
[3] Z. Huang, Z. Zhu, Z. Liu, Q. Liu, J. Catal. 214 (2003) 213–219.
[4] M. Stanciulescu, G. Caravaggio, A. Dobri, J. Moir, R. Burich, J.-P. Charland, P. Bulsink, Appl. Catal., B 123–124 (2012) 229–240.
[5] Y.J. Kim, H.J. Kwon, I. Heo, I.-S. Nam, B.K. Choa, J.W. Choung, M.-S. Cha, G.K. Yeo, Appl. Catal., B 126 (2012) 9–21.
[6] F.D. Liu, H. He, Y. Ding, C.B. Zhang, Appl. Catal., B 93 (2009) 194–204.
[7] M. Casapu, O. Kröcher, M. Elsener, Appl. Catal., B 88 (2009) 413–419.
[8] S. Yang, C. Wang, J. Li, N. Yan, L. Ma, H. Chang, Appl. Catal., B 110 (2011) 71–80.
[9] B. Thirupathi, P.G. Smirniotis, J. Catal. 288 (2012) 74–83.
[10] M. Wallin, S. Forser, P. Thormahlen, M. Skoglundh, Ind. Eng. Chem. Res. 43 (2004) 7723–7731.
[11] Z. Wu, B. Jiang, Y. Liu, H. Wang, R. Jin, Environ. Sci. Technol. 41 (2007) 5812–5817.
[12] Z. Wu, R. Jin, Y. Liu, H. Wang, Catal. Commun. 9 (2008) 2217–2220.
[13] M. Kang, E.D. Park, J.M. Kim, J.E. Yie, Catal. Today 111 (2006) 236–241.
[14] G. Qi, R.T. Yang, Appl. Catal., B 44 (2003) 217–225.
[15] J. Huang, Z. Tong, Y. Huang, J. Zhang, Appl. Catal., B 78 (2008) 309–314.
[16] W. Sjoerd Kijlstra, M. Biervliet, E.K. Poels, A. Bliek, Appl. Catal., B 16 (1998) 327–337.
[17] T.S. Park, S.K. Jeong, S.H. Hong, S.C. Hong, Ind. Eng. Chem. Res. 40 (2001) 4491–4495.
[18] Z. Liu, J. Li, A.S.M. Junaid, Catal. Today 153 (2010) 95–102.
[19] H. Chang, J. Li, X. Chen, L. Ma, S. Yang, J.W. Schwank, J. Hao, Catal. Commun. 27 (2012) 54–57.
[20] B. Shen, T. Liu, N. Zhao, X. Yang, L. Deng, J. Environ. Sci. 22 (9) (2010) 1447–1454.
[21] J. Yu, F. Guo, Y. Wang, J. Zhu, Y. Liu, F. Su, S. Gao, G. Xu, Appl. Catal., B 95 (2010) 160–168.
[22] C. Liu, L. Chen, J. Li, L. Ma, H. Arandiyan, Y. Du, J. Xu, J. Hao, Environ. Sci. Technol. 46 (2012) 6182–6189.
[23] Z. Wu, R. Jin, H. Wang, Y. Liu, Catal. Commun. 10 (2009) 935–939.
[24] Y. Wang, L. Yang, W.P. Liao, F. Wang, Adv. Mater. Res. 356–360 (2011) 529–532.
[25] T. Yamaguchi, T. Jin, K. Tanabe, J. Phys. Chem. 90 (1986) 3148–3152.
[26] M. Waqif, P. Bazin, O. Saur, J.C. Lavalley, G. Blanchard, O. Touret, Appl. Catal., B 11 (1997) 193–205.
[27] H. Mahzoul, L. Limousy, J.F. Brilhac, P. Gilot, J. Anal. Appl. Pyrolysis 56 (2000) 179–193.
[28] H. Abdulhamid, E. Fridell, J. Dawody, M. Skoglundh, J. Catal. 241 (2006) 200–210.
[29] W. Xu, H. He, Y. Yu, J. Phys. Chem. C 113 (2009) 4426–4432.
[30] D.A. Peña, B.S. Uphade, E.P. Reddy, P.G. Smirniotis, J. Phys. Chem. B 108 (2004) 9927–9936.
[31] H.K. Matralis, M. Ciardelli, M. Ruwet, P. Grange, J. Catal. 157 (1995) 368–379.
[32] L. Lietti, G. Ramis, F. Berti, G. Toledo, D. Robba, G. Busca, P. Forzatti, Catal. Today 42 (1998) 101–116.
[33] M.A. Larrubia, G. Ramis, G. Busca, Appl. Catal., B 27 (2000) L145–L151.
[34] M.A. Centeno, I. Carrizosa, J.A. Odriozola, Appl. Catal., B 29 (2001) 307–314.
[35] R.Q. Long, R.T. Yang, J. Catal. 190 (2000) 22–31.
[36] R.Q. Long, R.T. Yang, J. Catal. 207 (2002) 224–231.
[37] R. Jin, Y. Liu, Z. Wu, H. Wang, T. Gu, Catal. Today 153 (2010) 84–89.
[38] F. Liu, K. Asakura, H. He, W. Shan, X. Shi, C. Zhang, Appl. Catal., B 103 (2011) 369–377.
[39] M. Kantcheva, J. Catal. 204 (2001) 479–494.
[40] S. Xie, J. Wang, H. He, J. Mol. Catal. A: Chem. 266 (2007) 166–172.
[41] M. Machida, M. Uto, D. Kurogi, T. Kijima, Chem. Mater. 12 (2000) 3158–3164.
[42] T. Gu, R. Jin, Y. Liu, H. Liu, X. Weng, Z. Wu, Appl. Catal., B 129 (2013) 30–38.
[43] G. Xie, Z. Liu, Z. Zhu, Q. Liu, J. Ge, Z. Huang, J. Catal. 224 (2004) 36–41.
[44] B. Zhang, B. Chen, K. Shi, S. He, X. Liu, Z. Du, K. Yang, Appl. Catal., B 40 (2003) 253–258.
[45] I.S. Nam, J.W. Eldridge, J.R. Kittrell, Ind. Eng. Chem. Prod. Res. Dev. 25 (1986) 192–197.
[46] Y. Ji, T. Toops, M. Crocker, Catal. Lett. 127 (2009) 55–62.
[47] L. Kylhammar, P.-A. Carlsson, H.H. Ingelsten, H. Grönbeck, M. Skoglundh, Appl. Catal., B 84 (2008) 268–276.
[48] J. Ma, Z. Liu, Q. Liu, S. Guo, Z. Huang, Y. Xiao, Fuel Process. Technol. 89 (2008) 242–248.
[49] G.S. Qi, R.T. Yang, J. Phys. Chem. B 108 (2004) 15738–15747.
[50] G. Kresse, J. Furthmuller, Comput. Mater. Sci. 6 (1996) 15–50.
[51] G. Kresse, J. Furthmuller, Phys. Rev. B: Condens. Matter 54 (1996) 11169.